Int. J. Advanced Design and Manufacturing Technology, 2025, Vol. 18, No. 1, pp. 51-63

DOI: 10.71644/admt.2025.1185066 *ISSN: 2252-0406* *https://admt.isfahan.iau.ir*

Transient Vibration Analysis of an Optimized FML Cylindrical Shell Based on Maximum Reliability

Alireza Pourmoayed *
Department of Mechanical Engineering,
University of Khatamul-Anbiya Air Defense, Iran
E-mail: a.pourmoayed@khadu.ac.ir
*Corresponding author

Keramat Malekzadeh Fard
Department of Structural Analysis and Simulation, Aerospace Research Institute, University of Malek Ashtar, Iran
E-mail: kmalekzadeh@mut.ac.ir

Ali Nazari
Department of Aerospace Engineering, Aerospace Research Institute, Iran
E-mail: nazariali23@yahoo.com

Received: 26 September 2024, Revised: 23 December 2024, Accepted: 1 January 2025

Abstract: The transient vibration analyses of optimised Fibre Metal Laminates Cylindrical shells were examined in this paper. One of the most innovative aspects of this study is identifying an applied trend for optimizing the FML cylindrical shell construction to achieve maximum reliability. The FML shell reliability is determined using the First Order Reliability Method (FORM) and the Hashin failure criteria. To achieve this objective, the Shell is constantly subjected to a static load, and the resulting tensions within the FML layers of the shell are measured. The maximum tension is determined using the Hashin method, and the stability of the shell is subsequently estimated. Next, the amounts of reliability are certified according to shell stability. To maximize the FML shell reliability, the sequence of the composite-metal layers and fibre orientation are often modified, and for each case, the sample reliability is calculated. The second section of this study examines the effect of the optimized structure of the FML shells on the acceleration and displacement of these shells under dynamic loading. The energy approach is used to obtain the Equations of motion, whereas the mode superposition method is employed for transient vibration analysis.

Keywords: Fiber Orientation, FML Shell, Layup, Reliability, Transient Vibration

Biographical notes: **Ali Reza Pourmoayed** is an Associate Professor of Aerospace Engineering at the University of Khatamul-Anbiya Air Defence, Iran. He received his PhD in Airspace Engineering from Malek-Ashtar University of Technology in 2017. **Keramat Malekzadeh Fard** received his PhD in Mechanical Engineering from the University of K. N. Toosi in 2005. He is currently a Professor at the Department of Aerospace Engineering, Malek-Ashtar University of Technology, Tehran, Iran. **Ali Nazari** received his PhD from Aerospace Research Institute in 2019.

Research paper

1 INTRODUCTION

In general, industrial structures are subjected to dynamic loads, which can lead to vibration, buckling, or fatigue. One of the more useful parts of many transportation vehicles is the composite shell. One of the primary issues with these shells is that they will be significantly deformed under dynamic loads, which results in a perceptible reduction in the strength of composite shells. One of the methods that decreases this negative effect of dynamic loads is using of fiber metal laminates which are briefly called FML.

Many researchers have been done on the Transient vibration of composite cylindrical shells, for example, Lee et al. [1] analyzed the dynamic response of simply supported-simply supported Cross-Ply laminated circular cylindrical shells under impulse loads based on first-order shear deformation theory. They did not consider the pre-stress effect in the governing Equations of motion. Lam and Loy [2] examined the effects of boundary conditions on a slender rotating cylindrical shell made of layers using Love's first approximation and the Galerkin method. Chen [3] investigated the transient dynamic response analysis of an orthotropic circular cylindrical shell under external hydrostatic pressure. The researchers employed conventional shell theory and took into account the boundary requirements of simply supported. Karagiozova et al. [4] conducted a study on the transient deformation process of FMLs subjected to localized blast loading. They used the finite element method to analyze the deformation mechanism caused by highly localized pressure pulses, which result in permanent deformations and damage observed in FML panels during experiments. They demonstrated that the reaction of the FML panels is highly responsive to changes in the spatial and temporal distribution of pressure resulting from the blast loading. The study conducted by Khalil et al. [5] examined the dynamic behaviour of pre-stressed Fibre Metal Laminate (FML) circular cylindrical shells under lateral pressure pulse loads. The shell's equilibrium Equations were derived using the First-Order Shear Deformation Theory (FSDT), while the strain-displacement relations were based on Love's first approximation theory. The Galerkin method was employed to solve the equilibrium Equations for buckling, free vibration, and forced vibration problems of the shell.

Malekzadeh et al. [6] examined the Transient Dynamic response of multilayer circular cylindrical shells made of hybrid composite materials when exposed to a lateral impulse force. The boundary conditions are assumed to be clamped on one end and free on the other end. Both isotropic (metal) and orthotropic (composite) layers are used simultaneously in the hybrid Lamination. First-order shear deformation theory (FSDT) and Love's first approximation theory are utilized in the shell's equilibrium Equations. Equilibrium Equations for free and forced vibration problems of the shell are solved using Galerkin method. Finally, the time response of displacement components of Fiber-Metal Laminate (FML) cylindrical shells is derived using the mode superposition method. The non-linear dynamic instability of laminated composite cylindrical shells subjected to periodic axial loads is analyzed by Darabi et al. [7]. Dynamic instability of thin laminated composite cylindrical shells subjected to harmonic axial loading is investigated based on nonlinear analysis. The Equations of motion are developed using Donnell's shallow-shell theory and with von Karman-type nonlinearity. The nonlinear large deflection shallow-shell Equation of motions is solved by using Galerkin's technique that leads to a system of nonlinear Mathieu–Hill Equations.

Also, some research has been done on the optimization of composite cylindrical shells. For example, Haichao et al. [8] investigated the Simultaneous Optimization of Stacking Sequences and Sizing with Two-Level Approximations and a Genetic Algorithm. A new optimization model is first established by involving both stacking sequence and sizing variables. Within a single procedure, the genetic algorithm is used to solve a first-level approximate problem which includes both types of variables, while a second-level approximate problem is addressed for the individual fitness calculations. Numeric applications are presented to demonstrate the efficacy of this optimization strategy. Sen et al. [9] presented a Design optimization procedure for fiber metal laminates based on fatigue crack initiation. The state-of-the-art design method is a solution-oriented analysis, where only selected lay-ups are assessed for satisfying the design criteria. They aim to develop a reversed design procedure where the lay-ups are obtained as design solutions. Therefore, a genetic algorithm procedure is developed to find the optimal lay-up satisfying the required fatigue life. Ali Haeri et al. [10] presented the efficient reliability of laminated composites using an advanced Kriging surrogate model. To demonstrate a computationally efficient and accurate approach to the reliability analysis of laminated composites, an advanced Kriging model is applied to approximate the mechanical model of the structure. To construct the surrogate model, the structural response is simulated through the finite element method based on the classic theory of laminates. Tsai–Wu criterion is adopted to define limit state function in reliability analysis. A high-quality surrogate is achieved using a probabilistic classification function together with a metric for refinement of the model.

Malakzadeh Fard and Pourmoayed investigated the dynamic instability problem of beams built of Functionally Graded Materials (FGM) [11]. For this objective, the first-order shear deformation (or

Timoshenko) beam theory is examined in conjunction with the effects of geometric nonlinearity. The governing Equations, as well as various forms of common boundary conditions, are obtained by analyzing the energy functions of the system and applying Hamilton's principle. Ma et al. [12] focused on the dynamic analysis of FMLs, considering both macromechanical and micromechanical scale features. Additionally, the optimization studies on Fibre Metal Laminates (FMLs) within the context of dynamic analysis were investigated. The analysis and optimization of fibre-metal laminate cylindrical shells subjected to transverse impact loads were examined by Azarafza and Davar [13]. In order to achieve this objective, the genetic algorithms method is implemented to optimize the combination of the objective functions, which include weight and transverse impact response, as well as two constraints, which include critical buckling loads and principal strains.

The transient dynamic analysis of grid-stiffened composite conical shells is reviewed by Zamani et al. [14]. The influence of many parameters on forced vibrations has been studied, including fiber angle, geometric ratios, type, and so on. Also, this study examined the consequences of using grid-stiffened structures to strengthen the conical shell. Davar et al. [15] conducted a study on the reaction of laminated composite cylinder shells to low-velocity impacts under coupled pre-loads. Their findings revealed that regardless of the kind of axial pre-load (tensile or compressive), changes in contact characteristics during impact are linearly proportional to temperature changes. In addition, the changes in radial pressure are almost linear when there is a tensile axial pre-load, but they are nonlinear when there is a compressive axial pre-load. Alibeigloo and Talebitooti [16] conducted the study. The study examines the transient response of a cylindrical panel made of Functionally Graded Material (FGM) that is simply supported. The panel is equipped with sensor and actuator piezoelectric layers and is exposed to an electric field and thermal shock. The investigation is conducted using generalized coupled thermoelasticity, which is based on the Lord-Shulman theory. The study investigates the influence of a constant relaxation temperature, applied voltage, and thermal shock on the thermoelastic response of a cylindrical panel made of Functionally Graded Material (FGM). The parametric investigation revealed that the presence of material inhomogeneity has considerable effects on the coupled thermoelastic response of the hybrid FGM cylindrical panel. Khalili et al. [17] conducted a novel study on the dynamic analysis of a continuous SMA hybrid composite beam. The study considered the instantaneous phase transformation and material nonlinearity effects at any given moment for every point along the beam. This research and such analysis are conducted for the first time. The results revealed the accuracy of the proposed model and the corresponding solution algorithm. Additionally, the presence of hysteresis behaviour in shape memory alloys (SMAs) causes a damped response in both SMA hybrid composite beams and complete SMA beams.

Pourmoayed et al. [18] examined the characteristics of free vibrations in a sandwich structure with viscoelastic piezoelectric composite face sheets reinforced by Functionally Graded Carbon Nanotubes (FG-CNTs). The study utilized a new and enhanced higher-order sandwich panel theory and considered simply supported boundary conditions. The study examined the influence of key elements, including the length-to-thickness ratio, volume percentages of fibers, core thickness, elastic foundation, temperature and humidity variations, magnetic field, viscosity, and voltage, on the free vibration response of a sandwich structure. Fu and Hu [19] investigated the transient response of fibre metal laminated (FML) shallow spherical shells with interfacial damage under the influence of an unstable temperature field. The current model offers a highly efficient approach for conducting nonlinear dynamic analysis on composite laminated structures that have interfacial degradation and are exposed to transient temperature fields. The shell's displacements and stresses increase over time and remain constant when the temperature is at a constant level.

The current study is the first to optimize the structure of FML cylindrical shells, intending to achieve maximum reliability, by modifying the sequence of composite–metal layers and fibre orientation. The effectiveness of optimizing the FML structure on the dynamic response of FML shells is also being researched. The energy approach is employed for establishing the Equation of motion, whereas the mode superposition method is utilized for dynamic analysis. The Galerkin method is employed to solve the equilibrium Equations for transient vibration problems of the shell.

2 THEORY AND FORMULATION

2.1. Basic Assumptions

In this study to decrease negative effects of dynamic loads on the strength of the FML shell, an applied designing process is used for optimization of the FML shell’s structure based on maximum reliability. In the second part of this study, transient vibration of the FML shell structures which have the maximum and minimum reliability have been studied and acceleration and displacement of these structures due to applied dynamic load have been considered in all directions. Finally, the effect of optimized structure of the FML shells on the acceleration and displacement of these shells are

investigated. The significance of this study lies in the fact that electronic equipment can be installed on the shells of certain transportation vehicles. However, many of these electronic components are susceptible to acceleration resulting from high-frequency dynamic loads. Therefore, it is important to determine the acceleration and displacement of these shells caused by dynamic loads. Using the determined maximum acceleration in each direction, it is possible to use electronic equipment capable of withstanding these accelerations.

The applied dynamic load refers to a high-frequency sinusoidal load that is applied over a short duration. To optimize the FML cylindrical shell structure to reach maximum reliability, the sequence of the composite-metal layers and the composite layer orientation of the FML shell are regularly changed. Each sample is subjected to a consistent static load, and the resulting tension stresses in the FML shell layers are measured to determine the maximum tension stress. The stability of all the FML shell samples is determined by applying Hashin's failure criteria and considering the ultimate strength of the FML layer's material. After determining the stability of all samples, the first-order reliability method is used to determine the reliability of the system. At last, an optimum structure with maximum reliability will be chosen for the FML shell. In order to perform the explained process, a prepared MATLAB program was linked to the finite element ABAQUS software. Various shells with different layer sequences and fibre orientations are generated and analyzed during the optimization process. This comprehensive program is able to analyze the FML shells with various arrangements of composite–metal layers, fiber orientation, and boundary conditions. In this investigation, free-clamp boundary conditions are used on the edges.

The sample analyzed in this research is a six-layer FML shell consisting of two layers made of aluminium and four layers made of glass/epoxy. This work employs a laminate coding technique to define the FML laminates. The coding system of the FML shell consists of six layers, denoted as AL/GE-i-j, [m,n,o,k]. A case study of a laminate FML shell is defined by the variables: i=2, j=4, m=n=0, o=k=90, and AL/GE-2-4. In this shell, the second and fourth layers are constructed of aluminium, while the other layers are made of glass/epoxy. The fibre orientation of the layers is [0,0,90,90] degrees, respectively. AL is an abbreviation for aluminium, whereas GE stands for glass-epoxy. The arrangement of metal and composite layers, as well as the orientation of composite layers, in the FML shell are from the inside to the outside. An example of a 3-layer FML (Fibre Metal Laminate) shell consists of layers of AL/Glass-Epoxy/Glass-Epoxy with a [0/90] angle configuration. The interior surface is composed of aluminium, the second layer is made of glass/epoxy with a 0-degree angle, and the outside layer is built of glass/epoxy with a 90-degree orientation.

2.2. Procedure of Calculation of FML Shell Reliability

In this study, the Hashin yield criterion to calculate the FML shell stability was applied. Then the reliability of the shell using shell stability was determined. In composite shells, increasing the stress to more than critical stress causes imperfection rather than serious fracture because the yield stress should be greater than critical stress. With continued loading, the defect in composite shells expands inch by inch, causing the shell to crack. In this study, it is assumed that the fracture of one layer causes the fracture of the entire laminate, hence the top level of permitted loading is defined by the fracture of one layer. For reliability study, the initial step should be modeling the FML laminate shell in finite element software, then subjecting this shell to constant static load and calculating the stress of the matrix and fiber failure threshold for each layer.

For stress analysis, Abaqus software is used. In the second stage, this information is used for a Matlab program to generate β reliability criteria for each failure mode of fiber and matrix based on an algorithm explained in the next portions. Finally, the reliability of the shell is assessed using the normal distribution table and the reliability criterion.

In this article, g_f and g_m fiber and matric fracture criteria are respected. However, X_T, X_C, Y_T, Y_C, S are random basic variables. S is shear strength, Y_C is bearing strength along the vertical line of fiber, Y_T is tensile strength along the vertical line of fiber, X_C is bearing strength along of fiber, X_T is tensile strength along of fiber. Then, the laminate was modeled and analyzed in Abaqus software to derive fiber stress and matric fracture criterion.

2.2.1. Hashin Criteria

The Hashin method divides the failure criteria into four components in order to increase accuracy. These sections include fibers rupture and matrix in tension and compression force. The tensile rupture of fibres caused by shear stresses is equivalent to:

$$\left(\frac{\sigma_{11}}{X_T}\right)^2+\frac{{\sigma_{12}}^2+{\sigma_{13}}^2}{{\sigma_{12}}^2}=\begin{cases}\geq 1\, fail\\ \prec 1 Intact\end{cases} \quad (1)$$

Additionally, fibre compression rupture is:

$$\left(\frac{\sigma_{11}}{X_C}\right)^2=\begin{cases}\geq 1\, fail\\ < 1 Intact\end{cases} \quad (2)$$

Matrix tensile rupture in case of $\sigma_3+\sigma_2 \succ 0$ is:

$$\frac{\sigma_{22}^2+\sigma_{33}^2}{Y_T^2}+\frac{\sigma_{23}^2+\sigma_{22}\sigma_{33}}{S_{23}^2}+\frac{\sigma_{12}^2+\sigma_{13}^2}{S_{12}^2}=\begin{cases}\geq 1 fail\\ <1 Intact\end{cases} \quad (3)$$

For Matrix tensile rupture if $\sigma_3+\sigma_2 \prec 0$:

$$\left[\left(\frac{Y_C}{2S_{23}}\right)^2-1\right]\left(\frac{\sigma_{22}+\sigma_{33}}{Y_C}\right)+\frac{\sigma_{22}^2+\sigma_{33}^2}{4S_{23}^2}+\frac{\sigma_{23}^2+\sigma_{22}\sigma_{33}}{S_{23}^2}+\frac{\sigma_{12}^2+\sigma_{13}^2}{S_{12}^2}=\begin{cases}\geq 1 fail\\ <1 Intact\end{cases} \quad (4)$$

In the aforementioned Equations, σ_3 represents lateral shear resistance and is equivalent to the permissible shear tension in the (3-2) plane. Conversely, the permissible shear tension in the (3-1) plane can be regarded as equal to that in the (2-1) plane, denoted as S. The Hashin criteria under plane tension conditions in the tension coordinate system are represented in "Fig. 1", illustrating the principal directions of the material.

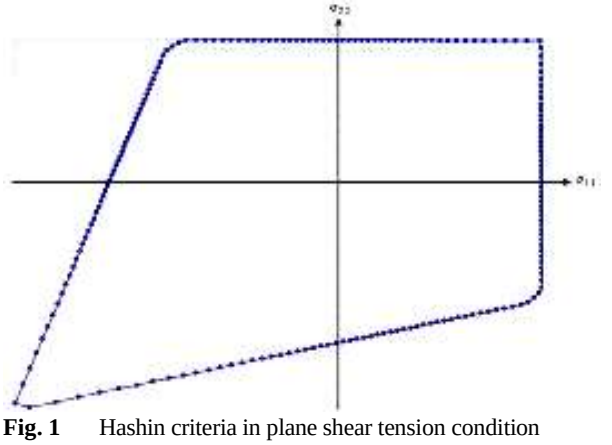

Fig. 1 Hashin criteria in plane shear tension condition

2.2.2. First Order Reliability Method

This work uses the first-order reliability method to calculate the reliability of FML shells. Some explanations for this strategy are presented as follows. The function G(X) is defined as an operation function, where $X=\left[X_1, X_2, ..., X_n\right]$ is a vector of random variables for this function. The region of g(x)>0 is a safe zone, the region of g(x) <0 is a failure zone and the region of g(x) =0 is a boundary zone. Reliability is defined as:

The probability of X random variables being in such a way that the operation function is in the safe zone (g(X)>0). If the probability density function of the X variable is $f_X(X)$, the probability of failure is defined as:

$$P_f = P\{g(X)<0\}=\int_{g(X)<0} f_x(x)dx \quad (5)$$

And reliability is calculated as:

$$R=1-P_f = P\{g(X)>0\}=\int_{g(X)>0} f_x(x)dx \quad (6)$$

The probability density function is typically nonlinear, and the integration limits of g(X) are multidimensional and nonlinear. Thus, the first-order reliability method uses intricate computations. These complex functions are the linear approximation of integration limits and the probability density function $f_X(X)$. Typically, tailor series are employed for these functions. The first-order reliability method is used from first-order multinomial for approximation. The first-order reliability method can be summarized as follows:

- Converting the main random variable from the x zone to the normal standard zone
- Search of MPP (Most Probable point) in U zone and calculating β reliability index
- Calculating reliability as follows:

$$R=\phi(\beta) \quad (7)$$

The choice of the probability density function can be made based on the nature of the problem, such as normal, lognormal, Weibull, gamma, etc.

2.2.3. Rosenblatt Transformation

This section presents the Rosenblatt Transformation. This function is utilized to attain reliability. In the first step, the random variable from the x zone, $X=\left\lfloor X_1, X_2, ..., X_n\right\rfloor$, should be transformed to standard normal zone. When the zone is changed, the probability density functions become regular. There are random variables in the U zone, $U=\left\lfloor U_1, U_2, ..., U_n\right\rfloor$, that follow a normal distribution. This transformation is true if the random variable cumulative distribution function is to be fixed after and before transformation. This transformation is named Rosenblatt Transformation.

Finally, the probability density function (PDF) for the normal distribution, denoted as ∅(U), has been obtained.

$$\phi_U(u)=\prod_{i=1}^{n}\frac{1}{\sqrt{2\pi}}\exp\left(-\frac{1}{2}u_i^2\right) \quad (8)$$

$$P_f=\int\int g(u_1,u_2,...,u_n)\prod_{i=1}^{n}\frac{1}{\sqrt{2\pi}}\exp\left(-\frac{1}{2}u_i^2\right)du_1du_2...du \quad (9)$$

3 PROCEDURES OF OPTIMIZATION OF FML CYLINDRICAL SHELL

The design variable in this study is the sequence of the

composite-metal layers and the fiber orientation of the composite layers in the FML cylindrical shell. The optimization goal is to achieve maximum reliability. Table 1 introduces the parameters of optimization.

Table 1 Introduction parameters used in the optimization process

Parameter name	Parameter definition
M	Number of metal layer of FML shell
N	Number of composite layers of FML shell
R	number of stances of fibers orientation for every layer
S	number of stances of composite–metal layers positioning order
U	number of total stances of fibers orientation for all of the composite layers
N.L.S	Number of considered layers sequences
N.L.U	Number of considered fibers orientation

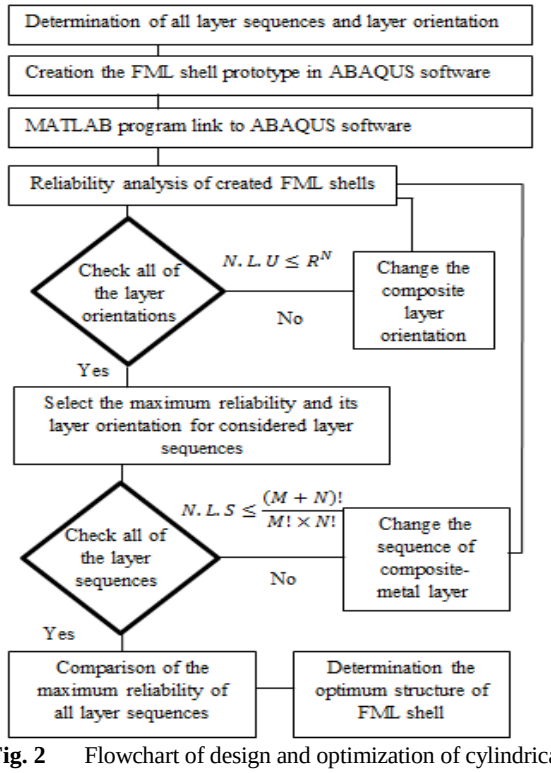

Fig. 2 Flowchart of design and optimization of cylindrical FML shell.

In order to optimize the performance, it is necessary to determine the number of positions for the composite-metal layers in the first step of the optimization method. For this purpose, "Eq. (10)" is used:

$$S = \frac{(M+N)!}{M! \times N!} \tag{10}$$

The number of fiber orientation stances of composite layers should be computed in the second stage using "Eq. (11)".

$$U = R^N \tag{11}$$

The total number of possible structures for an FML cylindrical shell with M metal layers and N composite layers can be found using "Eqs. (10) and (11)". Then, the optimum structure that causes the maximum reliability among all available structures should be determined. The flowchart of the design and optimization of the cylindrical FML shell is illustrated in "Fig. 2". The design constraints are as follows:

$$\begin{aligned} &\text{Maximize Reliability} \\ &0 < N.L.S \le \frac{(M+N)!}{M! \times N!} \\ &0 < N.L.U \le R^N \end{aligned} \tag{12}$$

4 GOVERNING EQUATIONS

The dynamic analysis of an optimized FML cylindrical shell employs the equilibrium Equations of the shell, using the First Order Shear Deformation Theory (FSDT) and Love's First Approximation Theory. The purpose of dynamic analysis is the calculated response of the shell under high-frequency sinusoidal load that is applied in a short time. Figure 3 shows a circular cylindrical shell with a mean radius of R, thickness h, and length L. The origin of the orthogonal coordinate system (X, φ, Z) is placed at the mid-surface at the end of the cylinder. The displacement of the cylinder in X φ and Z directions are defined by *u*,*v*, and *w*, respectively.

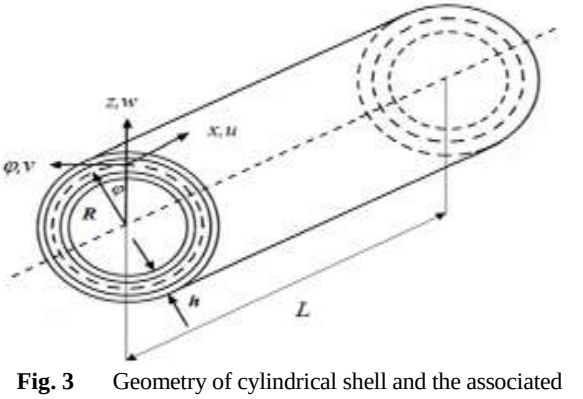

Fig. 3 Geometry of cylindrical shell and the associated coordinate system

The shell deformations are assumed to be small. According to first-order shear deformation theory, the equilibrium Equations for a cylindrical shell are as follows:

$$\begin{aligned}
&\frac{\partial N_x}{\partial x}+\frac{1}{R}\frac{\partial N_{x\varphi}}{\partial \varphi}=I_1\frac{\partial^2 u}{\partial t^2}+I_2\frac{\partial^2 \theta_x}{\partial t^2}\\
&\frac{\partial N_{x\varphi}}{\partial x}+\frac{1}{R}\frac{\partial N_\varphi}{\partial \varphi}+\frac{Q_\varphi}{R}=\left(I_1+\frac{2I_2}{R}\right)\frac{\partial^2 v}{\partial t^2}+\left(I_2+\frac{I_3}{R}\right)\frac{\partial^2 \theta_\varphi}{\partial t^2}\\
&\frac{\partial Q_x}{\partial x}+\frac{\partial Q_\varphi}{\partial \varphi}-\frac{N_\varphi}{R}+q_r\left(x,\varphi,t\right)=I_1\frac{\partial^2 w}{\partial t^2}\\
&\frac{\partial M_{x\varphi}}{\partial x}+\frac{\partial M_\varphi}{\partial \varphi}-Q_\varphi=\left(I_2+\frac{I_3}{R}\right)\frac{\partial^2 v}{\partial t^2}+I_3\frac{\partial^2 \theta_\varphi}{\partial t^2}\\
&\frac{\partial M_x}{\partial x}+\frac{\partial M_{x\varphi}}{\partial \varphi}-Q_x=I_2\frac{\partial^2 u}{\partial t^2}+I_3\frac{\partial^2 \theta_x}{\partial t^2}
\end{aligned} \tag{13}$$

In the above Equations θ_x and θ_φ are the slopes in planes of x-z and $\varphi-z$ respectively. Also q_r is the external force that excites the shell.

The correlations between the force resultants and the stress components of the shell are as follows:

$$\left(N_x,N_\varphi,N_{x\varphi},Q_x,Q_\varphi\right)=\int_{-\frac{h}{2}}^{\frac{h}{2}}\left(\sigma_x,\sigma_\varphi,\sigma_{x\varphi},\sigma_{xz},\sigma_{\varphi z}\right)dz \tag{14}$$

The relationship between the moment resultants and the stress components of the shell is as follows:

$$\left(M_x,M_\varphi,M_{x\varphi}\right)=\int_{-\frac{h}{2}}^{\frac{h}{2}}\left(\sigma_x,\sigma_\varphi,\sigma_{x\varphi}\right)zdz \tag{15}$$

In Equation (13), the mass inertia is defined by the following relation:

$$\left(I_1,I_2,I_3\right)=\int_{-\frac{h}{2}}^{\frac{h}{2}}\rho_k\left(1,z,z^2\right)dz \tag{16}$$

In "Eq. (16)", ρ_k is the density of each layer. Damping terms are excluded from the equilibrium Equations in the transient dynamic response analysis for the specified loading circumstances since the effect of structural damping is negligible. The stress-strain relations for a cylindrical shell are as follows:

$$\left\{\sigma_x,\sigma_\varphi,\sigma_{x\varphi},\sigma_{xz},\sigma_{\varphi z}\right\}^T=\left[\overline{Q_{ij}}\right]\left(\varepsilon_x,\varepsilon_\varphi,\varepsilon_{x\varphi},\varepsilon_{xz},\varepsilon_{\varphi z}\right)^T \;\&\; i,j=1,2,4,5,6 \tag{17}$$

$\overline{Q}_{ij}$ is the reduced stiffness matrix. The strain components in "Eq. (17)" are defined under Love's first approximation theory as follows:

$$\begin{aligned}
&\varepsilon_x=\varepsilon_x^0+z\kappa_x \qquad \varepsilon_\varphi=\varepsilon_\varphi^0+z\kappa_\varphi \qquad \varepsilon_{x\varphi}=\gamma_{x\varphi}^0+2z\kappa_{x\varphi}\\
&\varepsilon_{xz}=\gamma_{xz}^0 \qquad \varepsilon_{\varphi z}=\gamma_{\varphi z}^0
\end{aligned} \tag{18}$$

Strain and curvature are associated with the displacement component of the cylindrical shell according to Love's first approximation theory as follows:

$$\begin{aligned}
&\left\{\varepsilon_x^0,\varepsilon_\varphi^0,\varepsilon_{x\varphi}^0\right\}=\left\{\frac{\partial u}{\partial x},\frac{1}{R}\frac{\partial v}{\partial \varphi}+\frac{W}{R},\frac{1}{R}\frac{\partial u}{\partial \varphi}+\frac{\partial v}{\partial x}\right\}\\
&\left\{\kappa_x,\kappa_\varphi,\kappa_{x\varphi}\right\}=\left\{\frac{\partial \beta_x}{\partial x},\frac{1}{R}\frac{\partial \beta_\varphi}{\partial \varphi},\frac{1}{R}\frac{\partial \beta_x}{\partial \varphi}+\frac{\partial \beta_\varphi}{\partial x}\right\}\\
&\left\{\gamma_{xz}^0,\gamma_{\varphi z}^0\right\}=\left\{\beta_x+\frac{\partial W}{\partial x},\beta_\varphi+\frac{1}{R}\frac{\partial W}{\partial \varphi}-\frac{V}{R}\right\}
\end{aligned} \tag{19}$$

The boundary conditions for the cylindrical shell contain a combination of clamped and free conditions at its curving edges on both ends.

$$\begin{aligned}
&@\,x=L,N_x=\left(N_{x\varphi}+\frac{M_{x\varphi}}{R}\right)=\left(Q_x-\frac{\partial M_{x\varphi}}{R\partial x}\right)=M_x=0\\
&@\,x=0,u=v=w=\beta_x=\beta_\varphi=0
\end{aligned} \tag{20}$$

To fulfil the boundary conditions, u, v, w, β_x and β_φ are expressed by double Fourier series as follows:

$$\begin{aligned}
&u=\sum_m\sum_n A_{mn}\frac{d\eta_u\left(x\right)}{dx}\cos n\varphi T_{mn}\left(t\right)\\
&v=\sum_m\sum_n B_{mn}\eta_V\left(x\right)\frac{d}{dx}\sin n\varphi T_{mn}\left(t\right)\\
&w=\sum_m\sum_n C_{mn}\eta_w\left(x\right)\cos n\varphi T_{mn}\left(t\right)\\
&\beta_x=\sum_m\sum_n D_{mn}\frac{d\eta_{\beta_x(x)}}{dx}\cos n\varphi T_{mn}\left(t\right)\\
&\beta_\varphi=\sum_m\sum_n E_{mn}\eta_{\beta_x(x)}\sin n\varphi T_{mn}\left(t\right)\\
&\eta_{i(x)}=\alpha_1\cosh\frac{\lambda_m x}{L}+\alpha_2\cos\frac{\lambda_m x}{L}-\sigma_m\left(\alpha_3\sinh\frac{\lambda_m x}{L}-\alpha_4\sin\frac{\lambda_m x}{L}\right)\\
&\left(i=u,v,w,\beta_x,\beta_\varphi\right)
\end{aligned} \tag{21}$$

In "Eq. (21)", T_{mn} is the function of time, also, A_{mn}, B_{mn}, C_{mn}, D_{mn}, E_{mn} are the constant coefficients of the natural mode shapes. These numbers are related to the free vibration problem and are found by using the fact that mode shapes are orthogonal to the mass matrix. M is the axial half-wave number and n is the circumferential wave number. The values of α_i, σ_m and λ_m in "Eq. (21)" can be derived from the relevant boundary conditions.

5 TRANSIENT VIBRATION ANALYSES

This section defines external excitation and calculates the transient response of the acceleration and displacement components.

5.1. Definition of Dynamic Loading Condition

The term $q_r(x,\varphi,t)$ in "Eq. (13)" is the external force that excites the shell. The area of applied load $(2L_1 \times 2L_2)$ is variable and the coordinates of the center point of this area $(x_L \times \varphi_L)$ can be everywhere on the shell as:

$$\begin{aligned} &x_2 - x_1 = 2L_2 \quad R(\psi_2 - \psi_1) = 2L_1 \quad x_L = (x_2 + x_1)/2 \\ &\varphi_L = (\psi_2 + \psi_1)/2 \end{aligned} \tag{22}$$

The dynamic sinusoidal loading that stimulates the shell is delineated according to "Eq. (23)".

$$F(t) = 100\sin(5500t) \qquad 0 \le t \le 0.05 \tag{23}$$

The superposition approach is employed for dynamic analysis. This method transforms a continuous system into a discrete N-DOF linear system with a defined mode shape. The node displacement was characterised by the N component at an arbitrary time, with the u vector representing the node displacement. The Equations of motion are articulated by the mathematical statement provided in "Eq. (24)".

$$M\ddot{u}(t) + C\dot{u}(t) + ku(t) = p(t) \tag{24}$$

Where M is the mass matrix, *C* is the system viscous damping matrix and *K* is stiffness matrix in generalized coordinates U and p(t) is harmonic force and (.) denotes differentiation for time. The initial stage in a mode superposition solution involves determining the natural frequencies and natural modes of the system that fulfill the algebraic eigenvalue problem. The pivotal stage in the mode-superposition method is to implement the coordinate transformation.

$$u(t) = \sum_{m=1}^{N} \phi_m q_m(t) \tag{25}$$

The coordinates $q_m(t)$ will be referred to as principal coordinates or modal coordinates. "Eq. (25)" is substituted into "Eq. (24)" and the resulting Equation is multiplied by ϕ_m. To derive the Equation of motion in principal coordinates, solve "Eq. (26)" for each mode shape to determine the node displacement of the shell, using "Eq. (23)".

$$\sum_{m=1}^{N} M\phi_m \ddot{q}_m(t) + C\phi_m \dot{q}_m(t) + k\phi_m q_m(t) = p(t) \tag{26}$$

To solve the dynamic response issue, equilibrium Equations are incorporated into the strain-displacement and curvature-displacement relationships. Consequently, the resultant Equations may be expressed in the following manner:

$$\left[L_{ij} \right] \{u, v, w, \beta_x, \beta_\theta\} = \{0, 0, q_r, 0, 0\}^T \qquad ij = 1,....,5 \tag{27}$$

The applied impulsive load is defined as:

$$q_r(x,\varphi,t) = \sum_{m=1}^{\infty}\sum_{n=0}^{\infty} P_{mn} \sin\lambda x \cos n\varphi f(t) \tag{28}$$

In "Eq. (28)", $f(t)$ is function of time, P_{mn} is the constant Fourier coefficient that is calculated from the position, size, and profile of the applied load. The Galerkin method is employed to obtain a solution for "Eq. (27)".

6 VALIDATIONS OF THE RESULT

The mode convergence should be verified to ensure the validity of the result. In order to obtain the correct dynamic analysis response, the number of modes must be determined so that the structure response remains constant as the number of modes changes. This study assumes the maximum acceleration at the endpoint of the cylindrical shell in the w direction to evaluate the response convergence of the shell structure. In the current research, evaluating the response convergence for two distinct shell structures, the number of modes is set to 100, as increasing the number of modes beyond 100 does not change the structure's response. Figure 4 illustrates the convergence of responses from two distinct shells.

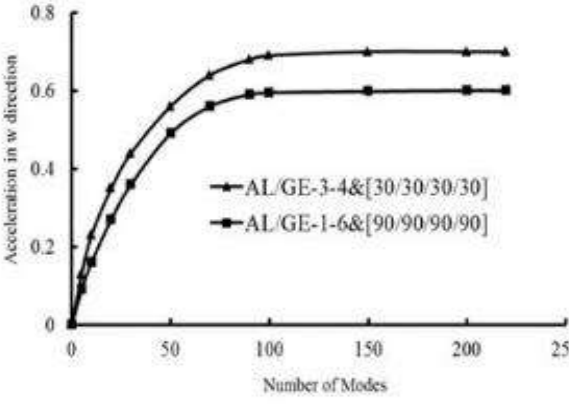

Fig. 4 Mode convergence plot

The validity and precision of the current study are

evaluated by comparing the results with the transient dynamic response of clamp-free hybrid composite circular cylindrical shells as presented by Malekzadeh and Khalili [6], illustrated in "Fig. 5". Dynamic analysis of a three-layer composite shell subjected to sinusoidal loading is taken into account for this purpose. Results are obtained for a clamped-free cylindrical shell with stacking sequence [45/0/45], the geometries of the considered shell are radius=2m, length =6m, and similar thickness for every layer=1mm. The material properties of the composite shell that was employed for the validation are demonstrated in "Table 2".

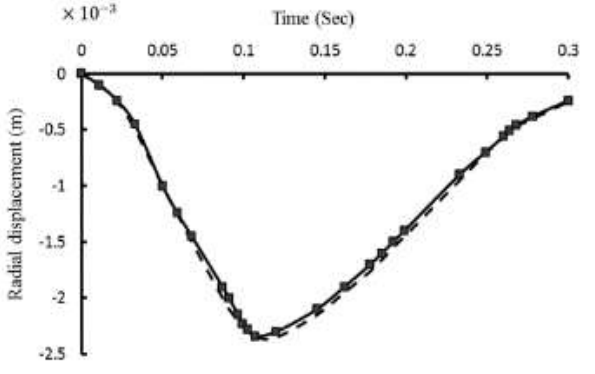

Fig. 5 Comparison of the dynamic analysis of composite shell (—■—present study,- - - Malekzadeh and Khalili [6]).

Table 2 Material properties used for composite shell for validation

ρ (kg/ m)	G12 (Gpa)	G23 (Gpa)	J_{12}	E_{22} (Gpa)	E_{11} (Gpa)
1643	4.1	1.3	0.26	7.6	19.0

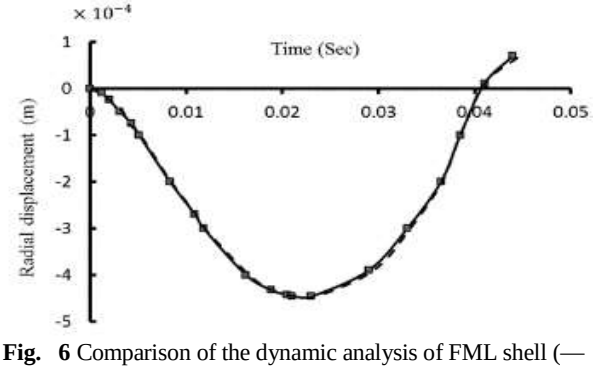

Fig. 6 Comparison of the dynamic analysis of FML shell (—■—present study,- - - Malekzadeh and Khalili [6]).

Additionally, a five-layer FML shell with a construction of AL/GFRP 0° / AL/GFRP 0° /AL] is considered for the validation of the dynamic response of the FML shell The results are compared with the transient dynamic response of clamp-free hybrid composite circular cylindrical shells as presented by Malekzadeh and Khalili [6]. In "Fig. 6", the geometries of the considered shell are radius=0.6m, length =2m, and similar thickness for every layer=2mm. Table 3 displays the material properties of the FML shell that was employed for this verification.

Table 3 Material properties used for FML shell for validation

material	ρ (kg/m^3)	G12 (Gpa)	G23 (Gpa)	J_{12}	E_{22} (Gpa)	E_{11} (Gpa)
GFRP	1390	1.8	0.69	0.35	5.1	14.34
Al 2024	2770	28	28	0.33	72.4	72.4

For this optimization process, an FML shell with two layers of aluminium and four layers of glass-epoxy is used. Table 4 shows the qualities of the material that was used to make this FML shell.

Table 4 Aluminum and glass/epoxy properties used for FML shells

material	density (kg/m^3)	Shear module (Gpa)	Poison ratio	Elastic module (Gpa)
Aluminum	$\rho = 2700$	G_{12}=27.8 G_{13}=27.8 G_{23}=27.8	$\vartheta_{12} = 0.3$ $\vartheta_{13} = 0.3$ $\vartheta_{23} = 0.3$	E_{11}=72.4 E_{22}=72.4 E_{33}=72.4
Glass-epoxy	$\rho = 2500$	G_{12}=4.7 G_{13}=4.7 G_{23}=3.28	$\vartheta_{12} = 0.25$ $\vartheta_{13} = 0.25$ $\vartheta_{23} = 0.42$	E_{11}=50 E_{22}=15.2 E_{33}=15.2

7 DETERMINATIONS OF SIX-LAYER FML SHELL OPTIMAL STRUCTURE UNDER CLAMP-FREE BOUNDARY CONDITION

Tables 5 and 6 present the maximum and minimum reliability indices, the corresponding maximum and minimum reliability values, and the fibre orientations that yield maximum and lowest reliability for all lay-up configurations of the six-layer FML shell.

The findings of the reliability analysis for the FML shell considered in this study, as presented in "Tables 5 and 6", indicate that the AL/GE-1-6 & [0/0/0/90] structure has the highest reliability, while the AL/GE-3-4 & [90/90/90/90] structure has the lowest reliability. Figure 7 shows the level of reliability for the best and worst structures of the FML cylindrical shells under consideration in this study.

Table 5 Comparison of the maximum reliability criteria and maximum reliability of clamp-free FML cylindrical shell for different kinds of layer sequences

Lay up	Maximum reliability criteria	Layer orientation that causes maximum reliability	Maximum reliability
AL/ GE-1-2	2.8611	0/0/0/90	99.77%
AL/ GE-1-3	2.7943	0/0/0/90	99.73%
AL/ GE-1-4	2.7957	0/0/0/90	99.74%
AL/ GE-1-5	2.8738	0/0/0/90	99.78%
AL/ GE-1-6	2.877	0/0/0/90	99.79%
AL/ GE-2-3	2.5763	90/0/0/90	99.50%
AL/ GE-2-4	2.577	90/0/0/90	99.50%
AL/ GE-2-5	2.7765	90/0/0/90	99.72%
AL/ GE-2-6	2.8122	90/0/0/0	99.75%
AL/ GE-3-4	2.5079	90/0/0/90	99.39%
AL/ GE-3-5	2.5369	90/0/0/90	99.44%
AL/ GE-3-6	2.7828	90/0/0/0	99.73%
AL/ GE-4-5	2.522	90/0/0/90	99.41%
AL/ GE-4-6	2.679	90/0/0/0	99.63%
AL/ GE-5-6	2.7889	90/0/0/0	99.73%

Table 6 Comparison of the minimum reliability criteria and minimum reliability of clamp-free FML cylindrical shell for different kinds of layer sequences

Lay up	Minimum reliability criteria	Layer orientation that causes minimum reliability	Minimum reliability
AL/ GE-1-2	1.3065	90/90/90/90	90.43%
AL/ GE-1-3	1.3072	90/90/90/90	90.44%
AL/ GE-1-4	1.3097	60/60/30/30	90.48%
AL/ GE-1-5	1.311	60/60/60/30	90.5%
AL/ GE-1-6	1.3131	60/60/60/30	90.54%
AL/ GE-2-3	1.2953	90/90/90/90	90.23%
AL/ GE-2-4	1.3034	90/90/90/90	90.37%
AL/ GE-2-5	1.3088	30/60/60/30	90.46%
AL/ GE-2-6	1.3107	60/60/60/30	90.5%
AL/ GE-3-4	1.2939	90/90/90/90	90.21%
AL/ GE-3-5	1.3064	90/90/90/90	90.42%
AL/ GE-3-6	1.3095	90/90/90/90	90.48%
AL/ GE-4-5	1.302	90/90/90/90	90.35%
AL/ GE-4-6	1.3081	90/90/90/90	90.45%
AL/ GE-5-6	1.3087	90/90/90/90	90.46%

Figure 8 shows the amount of reliability for four different layer sequences. It should be observed that the fibre orientation for the four different layer sequences depicted in "Fig. 8" is the same, specifically [60/30/0/90]. As can be seen in "Fig. 8", changing the fiber–metal layers sequence causes to high variation of shell reliability.

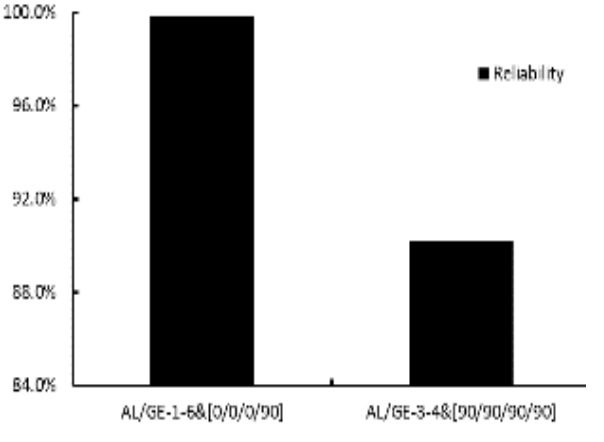

Fig. 7 Variation of reliability of FML cylindrical shell for the best and worst construction under free-clamp boundary conditions.

Figure 9 shows the effect of varying the composite layer orientation on the reliability of the FML shell under consideration in this work. Also, "Fig. 9" shows that changing the orientation of the composite layer has a small effect on the FML shell's reliability.

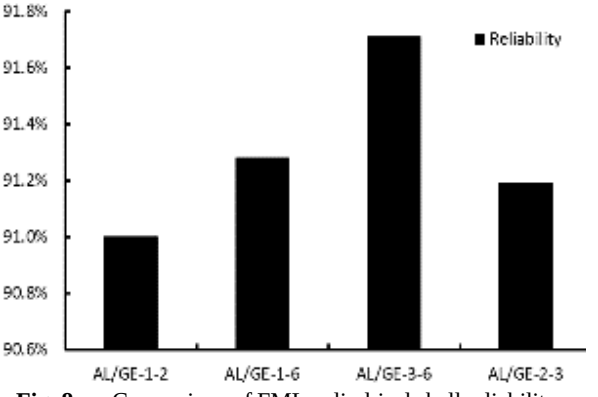

Fig. 8 Comparison of FML cylindrical shell reliability with [60,30,0,90] layup for four various layer sequences.

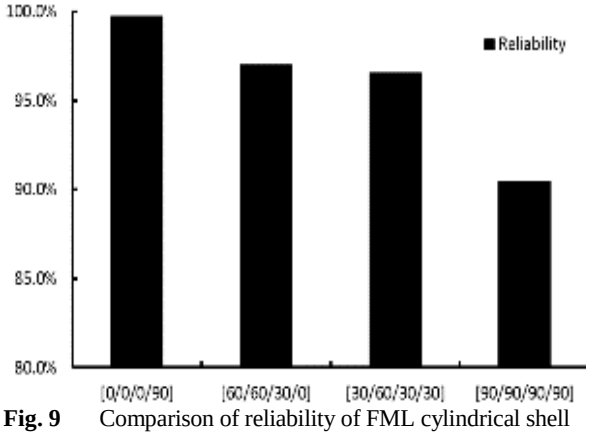

Fig. 9 Comparison of reliability of FML cylindrical shell with AL/GE-3-4-layer sequences for four various layer orientations.

The displacement variation of the best and worst FML shell structures under dynamic loading in the *u*, *v*, and *w* directions is shown in "Figs. 10-12" of this study.

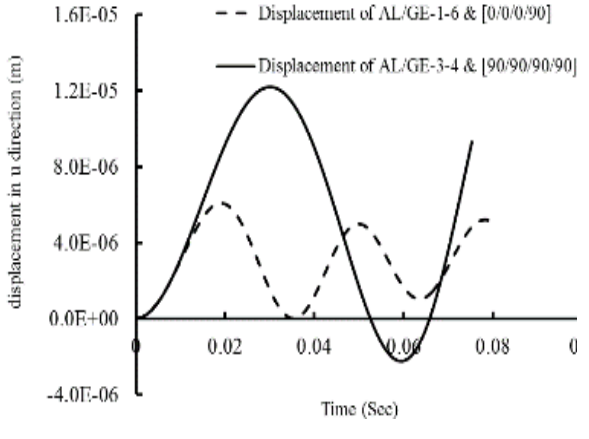

Fig. 10 Variation of displacement at the endpoint of FML cylindrical shell for the best and worst structure in the u direction.

Based on the data presented in "Fig. 10", it can be estimated that the displacement of the AL/GE-1-6 & [0/0/0/90] structure is approximately 130% smaller than that of the AL/GE-3-4 & [90/90/90/90] structure in the u direction. Based on the information shown in "Fig. 11", it can be inferred that the displacement of the AL/GE-1-6 & [0/0/0/90] structure is about 160% smaller than that of the AL/GE-3-4 & [90/90/90/90] structure in the vertical direction (v direction).

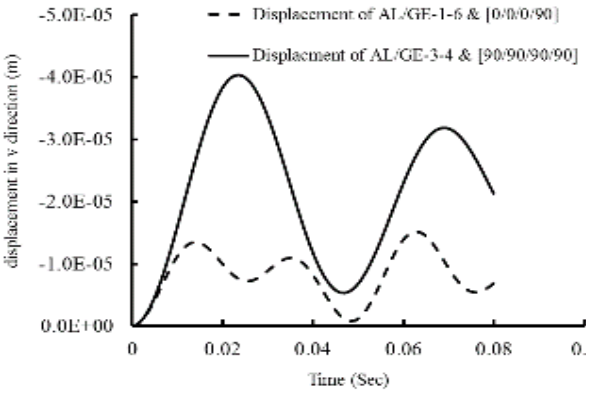

Fig. 11 Variation of displacement at the endpoint of FML cylindrical shell for the best and worst structure in v direction.

Figure 12 shows that the displacement of the AL/GE-1-6 & [0/0/0/90] structure in the w direction is approximately 130% smaller than that of the AL/GE-3-4 & [90/90/90/90] structure. Also, the analysis of Figures 10-12 indicates that optimizing the structure of the FML shell has a significant impact on the displacement of the FML shells when subjected to dynamic loading.

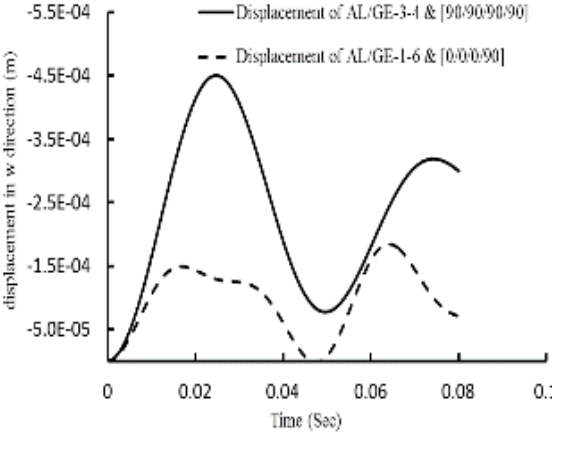

Fig. 12 Variation of displacement at the endpoint of FML cylindrical shell for the best and worst construction in w direction.

In this study, the FML shell's acceleration reaction in *u*, *v*, and *w* directions for the best and worst structures in terms of reliability is shown in "Table 7".

Table 7 Comparison of the acceleration at the endpoint of FML cylindrical shell for the best and worst structure in a) u, b) v, c) w directions

Shell structure	Maximum acceleration in u direction	Maximum acceleration in v direction	Maximum acceleration in w direction
AL/GE-1-6 & [0,0,0,90]	1.63e-6	6.75e-6	6.07e-8
AL/GE-3-4 & [90,90,90,90]	1.77e-6	7.03e-6	7.08e-8

Table 7 indicates that, in the u, v, and w directions, respectively, the acceleration of the AL/GE-1-6 & [0/0/0/90] structure is approximately %8, %4, and %16 less than that of the AL/GE-3-4 & [90/90/90/90] structure.

8 CONCLUSIONS

In this paper, transient vibration analyses of optimized Fiber Metal Laminates Cylindrical Shells were studied. Energy method is used to derive the Equations of motion and the mode superposition method is utilized for transient vibration analysis. The free-clamp boundary conditions are used on the edges in the present study. The first-order reliability method and Hashin failure criteria are used to determine the FML shell reliability. For this purpose, the shell is subjected to constant static load, and the resulting tensions within FML layers of the shell are measured. In the second part of this study, the effect of the optimized structure of the FML shells on the acceleration and displacement of these shells under dynamic loads are investigated. The results of this study can be summarized as follows:

- One of the most significant innovations of this work is the development of a valuable approach for optimising FML shells based on maximum reliability.
- A program is developed using MATLAB to optimise the performance. This program is coupled to the ABAQUS finite element software.
- The optimisation procedure of this study considers an FML shell consisting of 2 aluminium layers and 4 glass-epoxy layers. The best structure for maximum reliability is AL/GE-1-6 & [0/0/0/90], while the worst structure for minimum reliability is AL/GE-3-4 & [90/90/90/90].
- The displacement variation for the best and worst FML shell structures is illustrated in Figures 10, 11, and 12, corresponding to the u, v, and w directions, respectively. The figures indicate that optimising the FML shell structure significantly improves the displacement of these shells under dynamic loads.

REFERENCES

[1] Lee, Y., Lee, K. D., On the Dynamic Response of Laminated Circular Cylindrical Shells Under Impulse Loads, Journal of Computers & Structures, Vol. 35, 1997, pp. 149-57.

[2] Lam, K. Y., Loy, C. T., Influence of Boundary Conditions for A Thin Laminated Rotating Cylindrical Shells, Compos Struct, Vol. 41, 1998, pp. 215–28.

[3] Chen, Li., Transient Dynamic Response Analysis of Orthotropic Circular Cylindrical Shell Under External Hydrostatic Pressure, J Sound Vib, Vol. 257, 2002, pp. 967–76.

[4] Karagiozova, D., Langdon, G. S., Nurick, G. N., and Kim Yuen, C., Simulation of the Response of Fiber-Metal Laminates to Localized Blast Loading, Int. J. Impact Eng, Vol. 37, 2010, pp. 766-82.

[5] Khalili, S. M. R., Malekzadeh, and K., Davar, A., Dynamic Response of Pre-Stressed Fiber Metal Laminate (FML) Circular Cylindrical Shells Subjected to Lateral Pressure Pulse Loads, Journal of Composite Structures, Vol. 92, 2010, pp. 1308-17.

[6] Malekzadeh, K., Khalili, S. M. R., and Davar, A., Transient Dynamic Response of Clamp-Free Hybrid Composite Circular Cylindrical Shells, Journal of Apply Composite Material, Vol. 17, 2010, pp. 243-57.

[7] Darabi, M., Non-Linear Dynamic Instability Analyzes of Laminated Composite Cylindrical Shells Subjected to Periodic Axial Loads, Composite Structures, Vol. 147, 2016, pp. 168–84.

[8] Haichao, A., Chen, S., Huang, H., Simultaneous Optimization of Stacking Sequences and Sizing with Two-Level Approximations and A Genetic Algorithm, Composite Structures, Vol. 123, 2015, pp. 180–89.

[9] Sen, I., Alderliesten, R. C., and Benedictus, R., Design Optimization Procedure for Fiber Metal Laminates Based on Fatigue Crack Initiation, Journal of Composite Structures, Vol. 120, 2015, pp. 275-284.

[10] Haeri, A., Fadaee, M., Efficient Reliability Analysis of Laminated Composites Using Advanced Kriging Surrogate Model, Composite Structures, Vol. 149, 2016, pp. 26–32.

[11] Malakzadeh Fard, K., Pourmoayed, A., Dynamic Stability Analysis of FGM Beams Based on the Nonlinear Timoshenko Model, Journal of Computational Methods in Engineering, Vol. 42, 2023, pp. 63-76.

[12] Ma, Q., Merzuki, M. N. M., Rejab, M. R. M., Sani, M. S. M., and Zhang, B., A Review of The Dynamic Analysis and Free Vibration Analysis on Fiber Metal Laminates (FMLs), Functional Composites and Structures, Vol. 5. 2023, pp. 012003.

[13] Azarafza, R., Davar, A., Analysis and Optimization of Fibre-Metal Laminate Cylindrical Shells Subjected to

Transverse Impact Loads, AUT Journal of Mechanical Engineering, Vol. 4, 2020, pp. 535-52.

[14] Zamani, M., Davar, A., Beni, M. H., and Jam, J. E., Transient Dynamic Analysis of Grid-Stiffened Composite Conical Shells, Journal of Solid Mechanics, Vol. 14, 2022.

[15] Davar, A., Azarafza, R., Eskandari Jam, J., and Labbafian Mashhadi, A., Low-Velocity Impact Response Analysis of Laminated Composite Cylindrical Shells Subjected to Combined Pre-Loads, Journal of Stress Analysis, Vol. 6, 2021, pp. 139-56.

[16] Alibeigloo, A., Talebitooti, M., Three Dimensional Transient Coupled Thermoelasticity Analysis of FGM Cylindrical Panel Embedded in Piezoelectric Layers, Mechanics of Smart Structures, Vol. 1, 2020.

[17] Khalili, S. M., Dehkordi, M. B., and Shariyat, M., Modeling and Transient Dynamic Analysis of Pseudoelastic SMA hybrid composite beam, Applied Mathematics and Computation, Vol. 219, 2013, pp. 9762-82.

[18] Pourmoayed, A., Malakzadeh Fard, K., and Rousta, B., Free Vibration Analysis of Sandwich Structures Reinforced by Functionally Graded Carbon Nanotubes, Compos. Mater. Eng, Vol. 3, 2021, pp. 1-23.

[19] Fu, Y., Hu, S., Nonlinear Transient Response of Fibre Metal Laminated Shallow Spherical Shells with Interfacial Damage Under Unsteady Temperature Fields, Composite Structures, Vol. 106, 2013, pp. 57-64.